JOURNAL OF GUIDANCE, CONTROL, AND DYNAMICS
Vol. 33, No. 5, September–October 2010

Engineering Notes

Stationkeeping of a Flux-Pinned Satellite Network

Michael C. Norman* and Mason A. Peck†
Cornell University, Ithaca, New York 14853

DOI: 10.2514/1.49550

Nomenclature

C_r = rotational damping coefficient
C_t = translational damping coefficient
$\mathbf{d}$ = position vector relative to formation center of mass
$\mathbf{f}$ = vector representing an applied force
$\mathbf{I}$ = inertia dyadic
J = cost function
m = vehicle mass
n = number of vehicles
$\hat{\mathbf{n}}$ = unit vector normal to ideal formation plane
$\hat{\mathbf{n}}_{\mathrm{HTSC}}$ = unit vector normal to high-temperature superconductor surface
R = in-plane radial coordinate
$\mathbf{r}$ = position vector
$\boldsymbol{\tau}$ = vector representing an applied torque
$\mathbf{w}_\tau$ = input disturbance torque
$\mathbf{w}_f$ = input disturbance force
Z = out-of-plane displacement coordinate
θ_i = in-plane angular separation between vehicle i and $i+1$
$\boldsymbol{\mu}$ = vector representation of a magnetic dipole moment
$\boldsymbol{\mu}_0$ = vacuum permeability
$\boldsymbol{\omega}$ = angular velocity vector
$\mathbf{1}$ = identity dyadic
$\boldsymbol{\rho}$ = position vector relative to high-temperature superconductor

I. Introduction

SATELLITE formations offer the promise of meeting requirements for space systems that must achieve large spatial extents, such as large-aperture telescopes. Physically separating components enables long-baseline observations and a large collecting aperture without the weight associated with a truss support structure, and removing mechanical elements connecting individual satellites also introduces opportunities for modularization. These advantages in turn likely reduce launch costs, extend system life, and simplify repair operations [1]. However, by removing these mechanical connections entirely, we eliminate a simple and effective means of constraining the relative position among components, a disadvantage that the present study addresses.

Proposed means of overcoming this disadvantage focus mainly on active control, augmenting the dynamics of the system through additional physics, or a combination of the two. Through active control and independent inputs to the vehicles, a formation can maintain and modify relative positions and orientations of individual spacecraft, but typically necessitate near-constant or frequent actuation to counter environmental forces modifying the relative motion of the formation [2–4]. Natarajan and Schaub augment the natural dynamics of a two-vehicle formation in orbit by controlling the Coulomb force acting between electrically charged spacecraft and demonstrate the utility of such a control scheme for relative position maintenance [5]. Atchison and Peck propose specific types of formations made possible by using the Lorentz force on a charged object in orbit around a planet with a magnetic field as an input [6]. Ashun and Miller suggest a solution based on electromagnetic attraction among actively controlled magnetic fields [7]. The present study augments this list of possibilities by examining the feasibility of the flux-pinning effect between a magnetic field and a superconductor as a means of establishing an action-at-a-distance force. The primary advantage of using magnetic flux pinning over other approaches is that it creates a passively stable connection between two bodies, making active control of the relative spacecraft states an additional option instead of a necessity. Any solution based on magnetic attraction alonewhether achieved by permanent magnets or electromagnets cannot be described as passively stable. As a consequence of Earnshaws Theorem, active control is generally necessary for a system of magnetically interacting components to maintain relative position or follow an arbitrary path [8]. Conceptually, flux pinning sidesteps this issue by depending instead upon forces generated by current loops in the HTSC passively resisting change.

This reaction can be modeled as a multiple degree-of-freedom spring and damper with an equilibrium that corresponds to the pinned position and orientation relative to the source of a magnetic field [9,10]. In unactuated mechanical systems consisting of bodies interconnected by springs, masses, and dampers, the total energy of the system never increases, resulting in an asymptotically stable arrangement. By creating a similar arrangement in orbit, one can take advantage of this passively stable flux-pinning effect to establish a virtual structure that maintains relative position and orientation with reduced need for active control.

II. Flux-Pinning Effect

Motion of a magnetic field induces current vortices inside a high-temperature superconductor (HTSC), which then react to changes in the magnetic flux passing through the its surface [11,12]. The electrical resistance within the HTSC is negligible when the HTSC is below its so-called transition temperature. As a result, these vortices can persist indefinitely. This interaction establishes an equilibrium position and orientation of the magnetic field relative to the HTSC, in which perturbations are met with a restorative force. This force is hysteretic: its instantaneous direction and magnitude depend upon the history of relative movement [13]. For small motions, however, the flux-pinning reaction force resembles a linear, multiple degree-of-freedom spring-and-damper system. Small perturbations from the initial state result in reaction forces and torques characterized by stiffness and damping values derived by theory or experimentation [12,13]. One particularly important observation of flux-pinned magnet and superconductor pairs that can be verified through experiment is that there is no resistance to any rotations about an axis of symmetry in the magnet's magnetic field as these rotations do not change the flux passing through the HTSC surface [9,12].

Presented as Paper 2010-6475 at the AIAA Guidance, Navigation and Control Conference and Exhibit, Honolulu HA, 18–21 August 2008; received 22 February 2010; revision received 22 April 2010; accepted for publication 17 May 2010.

*Graduate Research Assistant, Department of Mechanical and Aerospace Engineering, 127 Upson Hall. Student Member AIAA.

†Assistant Professor, Department of Mechanical and Aerospace Engineering, 212 Upson Hall. Member AIAA.

There are many approaches to finding force and torque expressions that have been presented in recent literature [13–18]. Approaching the force and torque interaction from an analytical point of view is often complicated by a lack of a convenient manner in which to express the currents and their derivatives induced in the HTSC surface. Many of these analyses restrict motion to 1 degree of freedom, resulting in an absence in the literature of general, analytical expressions for the force and torque interaction required for analysis and simulation.

Kordyuk addresses this issue by developing a model of a magnet and semi-infinite superconductor pair that approximates the interaction through the sum of two conceptual magnetic fields embedded in the HTSC [19]. Figure 1 depicts the general concept of this model in the case of a magnetic dipole. This image model decomposes the external magnetic field of the HTSC into two components. The frozen image depends upon the magnetic field conditions when the HTSC passes its critical temperature. This process of cooling the superconductor in the presence of a magnetic field is termed *field-cooling*. The frozen image has a fixed position relative to the HTSC $\boldsymbol{\rho}_i^*$ that corresponds to the reflection of the relative position of the field-cooled dipole $\boldsymbol{\rho}_i$ over the HTSC surface. Its dipole moment vector $-\boldsymbol{\mu}_i^*$ is the reflection of the opposite of the field-cooled dipole moment vector $\boldsymbol{\mu}_i$, and is also fixed with respect to the HTSC. Similarly, the mobile image of the magnetic dipole has both a position $\boldsymbol{\rho}_c^*$ and dipole moment $\boldsymbol{\mu}_c^*$ corresponding to the reflections of the current relative position $\boldsymbol{\rho}_c$ and dipole moment vector $\boldsymbol{\mu}_c$ of the magnetic dipole over the HTSC surface. In combination, the magnetic fields generated by these two image dipoles establish a potential well that draws the permanent magnet back to its original field-cooled position and orientation.

This image model conveniently predicts forces and torques associated with a magnetic dipole interacting with a semi-infinite, planar HTSC suffering from no hysteresis or damping. As the magnetic field becomes more complex and the assumptions regarding the HTSC less applicable, the model suffers. However, Shoer and Peck demonstrate the validity of the image model supplemented by linear damping for predicting the stiffness of a low-mass magnet and superconductor pair for separation distances on the order of 10 cm [9,10].

Shoer observes that in cases where the magnetic field source and HTSC remain in the vicinity of their field-cooled locations, the damping force and torque due to hysteresis and other physical effects is approximately linear [10]. As the damping force applied between the HTSC and magnetic field source is internal to the system and cannot change the angular momentum sum, it is assumed to act along the relative separation vector between the objects. We also know that for a symmetric field, such as that for a dipole, rotations cause no torque about the axis of symmetry. Therefore, the damping torque applied is based on the relative angular velocity of the two objects projected onto a plane normal to the dipole moment vector. The damping coefficients of the interaction can be modified by the introduction of addition material, such as aluminum, to induce eddy current damping [10].

Combining these damping effects with the magnetic dipole interactions with the frozen and mobile dipole images results in the completed force and torque interaction description between the HTSC and magnetic dipole:

$$\mathbf{f}_m = \mathbf{f}(\boldsymbol{\rho}_c - \boldsymbol{\rho}_i^*, \boldsymbol{\mu}_c, -\boldsymbol{\mu}_i^*) + \mathbf{f}(\boldsymbol{\rho}_c - \boldsymbol{\rho}_c^*, \boldsymbol{\mu}_c, \boldsymbol{\mu}_c^*) - C_t \frac{\boldsymbol{\rho}_c \boldsymbol{\rho}_c}{\boldsymbol{\rho}_c \cdot \boldsymbol{\rho}_c} \cdot \dot{\boldsymbol{\rho}}_c \tag{1}$$

$$\mathbf{f}_h = -\mathbf{f}_m \tag{2}$$

$$\boldsymbol{\tau}_m = \boldsymbol{\tau}(\boldsymbol{\rho}_c - \boldsymbol{\rho}_i^*, \boldsymbol{\mu}_c, -\boldsymbol{\mu}_i^*) + \boldsymbol{\tau}(\boldsymbol{\rho}_c - \boldsymbol{\rho}_c^*, \boldsymbol{\mu}_c, \boldsymbol{\mu}_c^*) - C_r \left(\mathbf{1} - \frac{\boldsymbol{\mu}_c \boldsymbol{\mu}_c}{\boldsymbol{\mu}_c \cdot \boldsymbol{\mu}_c}\right) \cdot \boldsymbol{\omega}_{\mathrm{rel}} \tag{3}$$

$$\boldsymbol{\tau}_h = -\boldsymbol{\tau}_m - \boldsymbol{\rho}_c \times \mathbf{f}_m \tag{4}$$

Equations (1–4) depend upon the force and torque interactions between two magnetic dipoles. These relations are given in Landecker et al. [20] in terms of arbitrary vectors $\boldsymbol{\rho}$, $\boldsymbol{\mu}_a$, and $\boldsymbol{\mu}_b$:

$$\mathbf{f}(\boldsymbol{\rho}, \boldsymbol{\mu}_a, \boldsymbol{\mu}_b) = \frac{3\mu_0}{4\pi\rho^4}((\hat{\boldsymbol{\rho}} \times \boldsymbol{\mu}_a) \times \boldsymbol{\mu}_b + (\hat{\boldsymbol{\rho}} \times \boldsymbol{\mu}_b) \times \boldsymbol{\mu}_a - 2\hat{\boldsymbol{\rho}}(\boldsymbol{\mu}_a \cdot \boldsymbol{\mu}_b) + 5\hat{\boldsymbol{\rho}}(\hat{\boldsymbol{\rho}} \times \boldsymbol{\mu}_a) \cdot (\hat{\boldsymbol{\rho}} \times \boldsymbol{\mu}_b)) \tag{5}$$

$$\boldsymbol{\tau}(\boldsymbol{\rho}, \boldsymbol{\mu}_a, \boldsymbol{\mu}_b) = \frac{\mu_0}{4\pi\rho^3}(3(\hat{\boldsymbol{\rho}} \cdot \boldsymbol{\mu}_a)(\boldsymbol{\mu}_b \times \hat{\boldsymbol{\rho}}) + (\boldsymbol{\mu}_a \times \boldsymbol{\mu}_b)) \tag{6}$$

III. Application to Space Structures

Brown and Eremenko discuss the utility of a fractionated space system to generic mission operation concepts [1]. Flux pinning potentially provides a force to bind together vehicles with a spatial distribution, allowing the system to inherit some of the benefits of a fractionated architecture. The aim of implementing a flux-pinned connection between individual vehicles is to offer some degree of passive stability to the relative motion of the formation components. By pairing a HTSC on one vehicle with a magnetic field source on a second, we establish flux-pinning connections that tie the dynamics of a fractionated space system together. One critical design parameter for any flux-pinned noncontacting structure is the separation distance between the HTSC on one vehicle and the magnetic field source on its neighbor. Shoer and Peck demonstrated a strong dependence of the effective stiffness of the connection upon this distance [9,10], which in turn relates to the passive disturbance rejection capabilities of the system as a whole. While magnetic flux pinning with permanent magnets potentially provides sufficient passively stable dynamics for relative position and orientation states for a spacecraft formation,

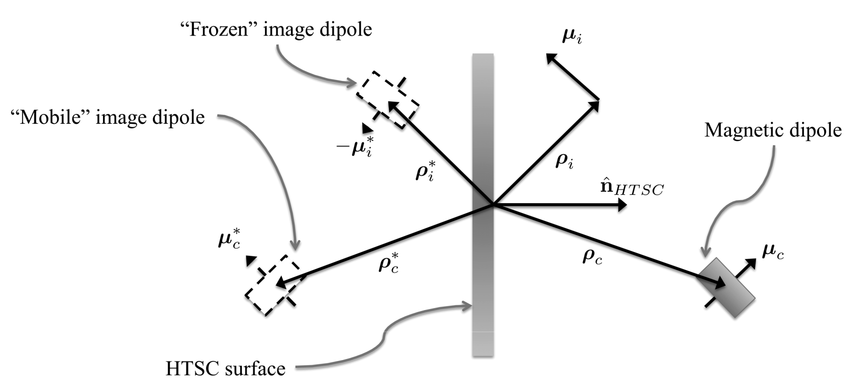

Fig. 1 Image-dipole model of flux pinning. The frozen and mobile dipole images are representative of the induced external magnetic field of the HTSC. The real magnetic dipole interacts with this field to impart a noncontacting force and torque.

Table 1 Ring vehicle parameters

Total mass, kg	100 kg
Bounding box dimensions, m^3	$1.0 \times 1.0 \times 0.2$
Principle moments of inertia, kg-m^2	[5.8 5.8 10.0]
Magnet location in body coordinates, m	[−0.5 0.0 0.0]
HTSC location in body coordinates, m	[0.5 0.0 0.0]
$\hat{\mathbf{n}}_{\text{HTSC}}$ in body coordinates	[1.0 0.0 0.0]
$\boldsymbol{\mu}_i$, $\boldsymbol{\mu}_c$ in body coordinates, J/T	[100.0 0.0 0.0]
C_t, Ns/m	0.01
C_r, Nms/rad	0.01

additional incorporation of an active feedback control law would further expand the reconfiguration and disturbance rejection capabilities of the formation. The literature describes several feedback control schemes specific to a particular noncontacting force that could be adapted for use with spacecraft dynamically linked by magnetic flux pinning [5,7].

Applying this simplified stiffness and damping model to a close-proximity formation of vehicles allows for preliminary investigations of the utility of flux pinning for space applications as a passive station-keeping effect. The example formation chosen is that of a noncontacting ring structure. This particular formation geometry is of interest in the development of sparse-aperture space telescopes

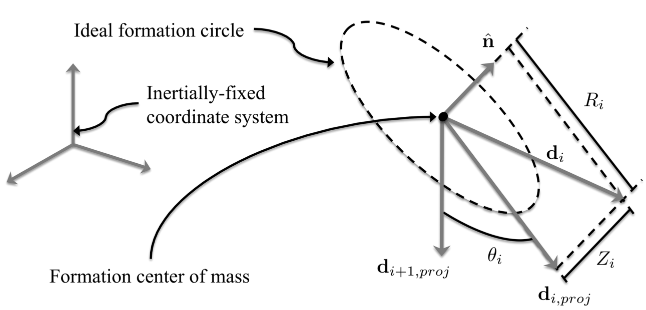

Fig. 2 Parameters used to determine the relative position of a vehicle to its ideal location on a ring in a plane.

and affords a few key advantages such as redundant UV-plane coverage [21].

The following simulations make a number of assumptions regarding the dynamics of the formation. All vehicles are assumed identical with a single HTSC and a single magnetic dipole, which interact via flux pinning with the two closest neighboring vehicles. The simulation treats the formation as free-floating, corresponding to a scenario where the formation is far from any significant gravitational field source. The resulting equations of motion for the ith vehicle is then

$$\mathbf{I}_i \cdot \dot{\boldsymbol{\omega}}_i = -\boldsymbol{\omega}_i \times \mathbf{I}_i \cdot \boldsymbol{\omega}_i + (\boldsymbol{\tau}_{m/i+1} + \mathbf{b}_m \times \mathbf{f}_{m/i+1}) + (\boldsymbol{\tau}_{h/i-1} + \mathbf{b}_h \times \mathbf{f}_{h/i-1}) + \mathbf{w}_{\tau i} \tag{7}$$

$$m_i \ddot{\mathbf{r}}_i = \mathbf{f}_{m/i+1} + \mathbf{f}_{h/i-1} + \mathbf{w}_{fi} \tag{8}$$

The first scenario consists of the candidate ring formation in the presence of input force and torque disturbances with no forces acting between the satellites. The second introduces a flux-pinned connection between neighboring vehicles. The input disturbance in both cases is modeled with a zero-mean Gaussian distribution with a standard deviation of 1-μN for the force disturbance and 1 μN-m for the torque disturbance as a nominal environmental effects of the same order of magnitude as some nonconservative perturbations, such as solar radiation pressure [22]. Table 1 lists the inertia properties and physical dimensions of each of the identical vehicles. In this scenario, 10 vehicles on a planar 3.6 m diameter ring, resulting in 16.14 cm separations between HTSC and magnetic dipoles on neighboring vehicles. Linearizing the dynamics of the system about the nominal ring formation predicts the damped natural frequencies of the structural modes associated with flux pinning to range between 0.00423 and 0.140 Hz. As the stiffness of the flux-pinned connection between vehicles depends upon the separation distance between the magnet and the HTSC [10], the natural frequencies of these modes can be shifted by defining a different ring diameter, and thus vehicle separation, as the equilibrium.

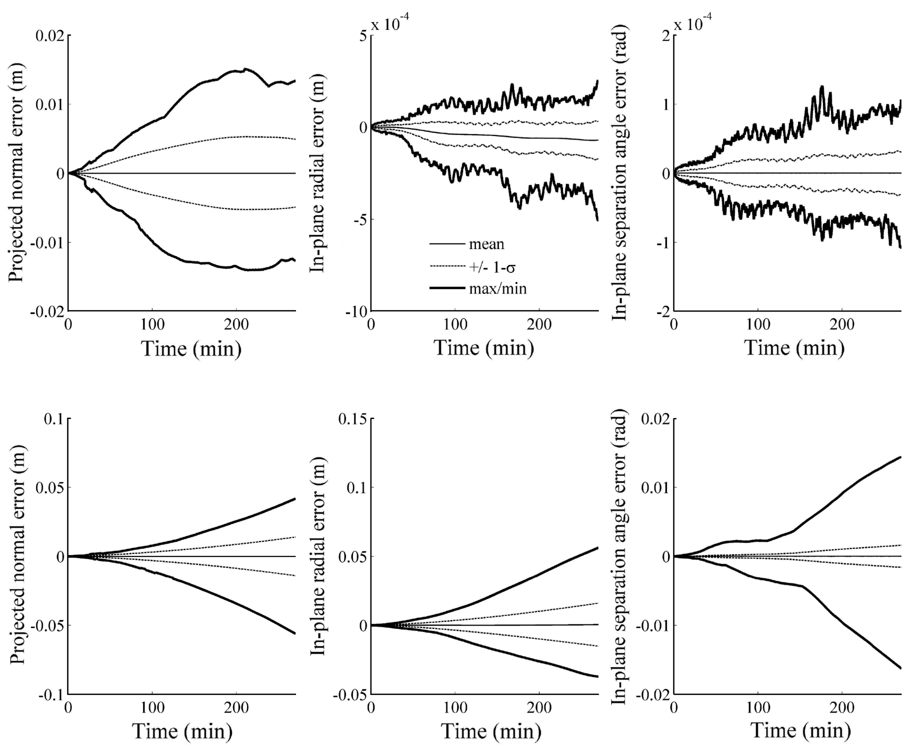

Fig. 3 Plots of the mean, $\pm 1 - \sigma$ bounds, and minimum/maximum values of vehicle position error of the 30 sets of both flux-pinned and dynamically unlinked formations as a result of disturbance forces and torques. The top row of plots correspond to the simulations with flux-pinning interfaces between neighboring vehicles. The bottom row of plots correspond to the unlinked simulations.

We aim to study the natural behavior of the system due to disturbance inputs in the absence of control. As the sum of the forces and torques due to noise tend to translate the system center of mass and overall orientation, performance parameters of the uncontrolled structure should depend only upon the relative motion of the vehicles. One such set of parameters would be the location of the vehicles relative to the formation center of mass in coordinates minimizing the out-of-plane position of the vehicles as is shown in Fig. 2. This plane passing through the formation center of mass has a normal vector $\hat{\mathbf{n}}$ that minimizes the following cost function:

$$J = \sum_{i=1}^{n} \frac{1}{2} (\hat{\mathbf{n}} \cdot \mathbf{d}_i)^2 = \frac{1}{2} \hat{\mathbf{n}}^T \left[\sum_{i=1}^{n} \mathbf{d}_i \mathbf{d}_i^T \right] \hat{\mathbf{n}}, \quad \text{where } \hat{\mathbf{n}}^T \hat{\mathbf{n}} = 1 \tag{9}$$

The coordinates Z_i, R_i, and θ_i depicted in Fig. 2 describe the position of the ith spacecraft in cylindrical coordinates with respect to the center of the formation located by $\mathbf{r}_{\mathrm{cm}}$. These measurements correspond to the out-of-plane displacement Z_i, the in-plane radial distance to the center of mass R_i, and the in-plane angular separation θ_i between vehicles i and $i+1$

$$Z_i = \mathbf{d}_i^T \hat{\mathbf{n}} \tag{10}$$

$$R_i = \sqrt{\mathbf{d}_i^T \mathbf{d}_i - Z_i^2} \tag{11}$$

$$\theta_i = \cos^{-1} \left(\frac{\mathbf{d}_i^T \mathbf{d}_{i+1} - Z_i Z_{i+1}}{R_i R_{i+1}} \right) \tag{12}$$

We performed 30 simulations of the ring formation for both the flux-pinned and dynamically-unlinked scenarios corresponding to unique disturbance input time histories. The means and standard deviations of these metrics over all 30 pairs of simulations are given in Fig. 3.

IV. Conclusions

Simulations of a 3.6 m ring formation of 10 vehicles with flux pinning acting between neighboring vehicles confirm that a flux-pinning interface can maintain a loose ring shape in the presence of input force and torque disturbances applied to the vehicles individually. The slight decrease in mean ring radius for the flux-pinned formation simulations is attributed to the projection of the relative position vector of the vehicles into a single plane. As expected, the noninteracting simulations resulted in a rapidly increasing radial position error and wider distribution of the vehicles in the out-of-plane direction. The resulting spatial formation of the vehicles for the noninteracting simulations had no resemblance to the original formation, especially in comparison to the loose ring maintained by the flux-pinned simulations. While the flux-pinning force and torque interaction between vehicles passively kept the formation together in a bulk sense, active control would be necessary for any task with strict relative position requirements.

References

[1] Brown, O., and Eremenko, P., "The Value Proposition For Fractionated Space Architectures," AIAA Paper 2006-7506, Sept. 2006.

[2] Inalhan, G., Tillerson, M., and How, J. P., "Relative Dynamics and Control of Spacecraft Formations in Eccentric Orbits," *Journal of Guidance, Control, and Dynamics*, Vol. 25, No. 1, Jan.–Feb. 2002, pp. 48–59.
doi:10.2514/2.4874

[3] Hamel, J.-F., and de Lafontaine, J., "Neighboring Optimum Feedback Control Law for Earth-Orbiting Formation-Flying Spacecraft," *Journal of Guidance, Control, and Dynamics*, Vol. 32, No. 1, 2009, pp. 290–299.
doi:10.2514/1.32778

[4] Ulybyshev, Y., "Long-Term Formation Keeping of Satellite Constellations Using Linear-Quadratic Controller," *Journal of Guidance, Control, and Dynamics*, Vol. 21, No. 1, Jan.–Feb. 1998, pp. 109–115.
doi:10.2514/2.4204

[5] Natarajan, A., and Schaub, H., "Linear Dynamics and Stability Analysis of a Two-Craft Coulomb Tether Formation," *Journal of Guidance, Control, and Dynamics*, Vol. 29, No. 4, Aug. 2006, pp. 831–838.
doi:10.2514/1.16480

[6] Atchison, J. A., and Peck, M. A., "A Millimeter-Scale Lorentz-Propelled Spacecraft," AIAA Paper 2007-6847, Aug. 2007.

[7] Ashun, U., and Miller, D. W., "Dynamics and Control of Electromagnetic Satellite Formations," *Proceedings of the 2006 American Control Conference*, IEEE, Minneapolis, MN, June 2006, pp. 1730–1735.

[8] Earnshaw, S., "On the Nature of the Molecular Forces which Regulate the Constitution of the Luminiferous Ether," *Transactions of the Cambridge Philosophical Society*, Vol. 7, No. 1, 1842, pp. 97–112.

[9] Shoer, J., and Peck, M., "Stiffness Of A Flux-Pinned Virtual Structure For Modular Spacecraft," *Journal of the British Interplanetary Society*, Vol. 62, No. 2, February 2009, pp. 57–65.

[10] Shoer, J. P., "Flux-Pinned Interfaces for the Assembly, Manipulation, and Reconfiguration of Modular Space Systems," *Proceedings of the 2008 AIAA Guidance, Navigation and Control Conference and Exhibit*, AIAA, Honolulu, HA, Aug. 2008.

[11] Hellman, F., Gyorgy, E. M., Johnson, D. W., O'Bryan, H. M., and Sherwood, R. C., "Levitation of a Magnet over a Flat Type II Superconductor," *Journal of Applied Physics*, Vol. 63, No. 2, 1988, p. 447.
doi:10.1063/1.340262

[12] Brandt, E. H., "Friction in Levitated Superconductors," *Applied Physics Letters*, Vol. 53, No. 16, 1988, p. 1554.
doi:10.1063/1.100435

[13] Chang, P.-Z., Moon, F. C., Hull, J. R., and Mulcahy, T. M., "Levitation Force and Magnetic Stiffness in Bulk High-Temperature Superconductors," *Journal of Applied Physics*, Vol. 67, No. 9, 1990, pp. 4358–4360.
doi:10.1063/1.344927

[14] Hull, J. R., and Cansiz, A., "Vertical and Lateral Forces Between a Permanent Magnet and High- Temperature Superconductor," *Journal of Applied Physics*, Vol. 86, No. 11, 1999, pp. 6396–6404.
doi:10.1063/1.371703

[15] Johansen, T. H., Mestl, H., and Bratsberg, H., "Investigation of the Lateral Magnetic Force and Stiffness Between a High-TC Superconductor and Magnet of Rectangular Shapes," *Journal of Applied Physics*, Vol. 75, No. 3, February 1994, pp. 1667–1670.
doi:10.1063/1.356351

[16] Tsuchimoto, M., Kojima, T., Takeuchi, H., and Honma, T., "Numerical Analyses of Levitation Force and Flux Creep on High TC Supercondutor," *IEEE Transactions on Magnetics*, Vol. 29, No. 6, Nov. 1993, pp. 3577–3579.

[17] Yamachi, N., Nishikawa, T., Sakai, N., Sawa, K., and Murakami, M., "Levitation Forces of Bulk Superconductors in Varying Fields," *Physica C: Superconductivity and Its Applications (Amsterdam)*, Vols. 392–396, Oct. 2003, pp. 579–584.
doi:10.1016/S0921-4534(03)01344-3

[18] Yang, Z. J., and Hull, J. R., "Effect of Size on Levitation Force in a Magnet/Superconductor System," *Journal of Applied Physics*, Vol. 79, No. 6, 1996, pp. 3318–3322.
doi:10.1063/1.361232

[19] Kordyuk, A. A., "Magnetic Levitation for Hard Superconductors," *Journal of Applied Physics*, Vol. 83, No. 1, Jan 1998, pp. 610–613.
doi:10.1063/1.366648

[20] Landecker, P. B., Villani, D. D., and Yung, K. W., "An Analytic Solution for the Torque Between Two Magnetic Dipoles," *Magnetic and Electrical Separation*, Vol. 10, No. 1, 1999, pp. 29–33.

[21] Meinel, A. B., and Meinel, M. P., "Large Sparse-Aperture Space Optical Systems," *Optical Engineering*, Vol. 41, No. 8, 2002, pp. 1983–1994.

[22] Vallado, D. A., *Fundamentals of Astrodynamics and Applications*, Microcosm Press, Hawthorne, CA, 2007, pp. 574–578, chap. 8.